Quasi-static FEA model for a multi-material soft pneumatic actuator in SOFA

Pasquale Ferrentino[1*], Antonio López-Díaz[2*], Seppe Terryn[1], Julie Legrand[1], Joost Brancart[3], Guy Van Assche[3], Ester Vázquez[4], Andrés Vázquez[2] and Bram Vanderborght[1]

1) Brubotics, Vrije Universiteit Brussel and Imec, Pleinlaan 2, 1050 Elsene, Belgium.

2) ETS Ingeniería Industrial, Universidad de Castilla-La Mancha, 13071 Ciudad Real, Spain.

3) Physical Chemistry and Polymer Science, Vrije Universiteit Brussel, Pleinlaan 2, 1050 Elsene, Belgium.

4) Inst. Regional Investigación Científica Aplicada, Universidad de Castilla-La Mancha, 13071 Ciudad Real, Spain.

***Abstract*—The increasing interest in soft robotics has led to new designs that exploit the combination of multiple materials, increasing robustness and enhancing performance. However, the combination of multiple non-linear materials makes modelization and eventually control of these highly flexible systems challenging. This article presents a methodology to model multi-material soft pneumatic actuators using finite element analysis (FEA), based on (hyper)elastic constitutive laws fitted on experimental material characterisation. The model in SOFA, the FEA software, allows to model and control in real-time soft robotic structures. One of the novelties presented in this paper is the development of a new user-friendly technique for the mesh partitioning in SOFA, using MATLAB algorithms, that allow the creation of uniform and more refined meshes and a mesh domain partitioning that can be adapted for any geometry. As a case study, a cylindrical multi-material soft pneumatic actuator is considered. It is composed of an internal chamber, which is constituted of an autonomous self-healing hydrogel, modelled as a hyperelastic material, and an external elastic reinforcement, made of thermoplastic polyether-polyurethane elastomer (TPPU), approached as a linear elastic material. The simulation of the combination of a hyperelastic and a linear elastic material in a single design is another contribution of this work to the scientific literature of SOFA simulations. Finally, the multi-material model obtained with the new mesh partitioning technique is simulated in quasi-static conditions and is experimentally validated, demonstrating an accurate fit, between simulation and reality.**

***Index Terms*—Soft robotics; multi-material; finite element method; FEA based control; self healing robots;**

I. Introduction

Soft robotics is a research field that is evolving fast, in fact, novel designs and control strategies for soft arms and actuators are continuously proposed in scientific literature [1]. The development of soft robots designs is focused on creating more robust and better performing robotic structures. One approach to this challenge is to exploit the combination of multiple materials in *multi-materials* robotic structures [2]. Varying the stiffness throughout the design can create complex anisotropic actuation responses [3], [4] and has shown to be useful in different soft robotics applications, including increasing the bending performance of actuators in soft grippers with robust grasps, in hand rehabilitation devices [5] and in joints of walking robots [6]. One of the principal reasons why multi-materials soft robotic designs are still challenging, is the strength at the *interface* between two different materials that are locally joined. In fact, if the two materials do not create strong bonds between each other, the interface results as the weakest point in the multi-material structure which is susceptible to rupture, due to the presence of stress concentrations and weak secondary bonds that provide limited adhesion [7]. Consequently, many multi-material soft robots have a limited lifetime, leading to non-optimal economical and ecological solutions.

Recent use of *smart materials*, in particular self-healing polymers, in the soft robotics field has tackled this problem, increasing the robustness by creating healable soft robots [8], [9]. Self-healing materials have the particular ability to recover from macroscopic damages without losing mechanical performance. As they are composed of reversible crosslinks, they can be manufactured and reprocessed via a wide varieties of manufacturing techniques [10]. Multiple self-healing polymers can be assembled together [11], [12] or with other non self-healing parts [13], creating multi-material structures with a higher degree of anisotropic deformation response, resulting in more complex actuation modes. Consequently, this type of materials offers a big opportunity for soft robotic research, permitting to create mechanical structures with a high degree of *embodied intelligence*, while at the same time increasing the lifetime of the robotic systems healing [14]. By adapting the polymer network composition, the mechanical properties of many of these self-healing polymers can be fine tuned onto specific requirements imposed by a specific application [15], providing excellent degree of freedom in the design of multi-material soft robots.

However, multi-material design has an impact on the modelling and control of soft robots, increasing its complexity. Although, multiple model-based strategies have been published, like the *Constant Curvature* (CC) model [16] and *Piecewise Constant Curvature* (PCC) model [17] based on *modified Denavit-Hartenberg parameters*, used for multi-section manipulators that have large non-planar motions. Recent developments of this techniques leads to the creation of kinematic [18] and dynamic controllers [19], that involves also contacts with the environments. These methods are governed by a lot of

*Both contributed equally to this work. Corresponding authors emails: pasquale.ferrentino@vub.be and antonio.ldiazcampo@uclm.es

assumptions and analytical equations, like in [20], they show lack of accuracy, as demonstrated in [21] and almost all are limited to single material designs. Other research groups rely on model-free strategies, like [22], [23], but they don't retrieve any mechanical relation between the material and the actuator level, that is the approach pursued in this scientific article.

In fact, this research work follows a methodology for material-based modelling of soft robots, introduced in [24] and expands it towards multi-material modelling (Fig. 1). The methodology is based on finite element analysis (FEA) in the SOFA environment [25], which allows to model and control soft pneumatic actuators [26] and manipulators [27]. SOFA has multiple limitations when it comes to modeling multi-material soft robots, which will be addressed in this paper. Firstly, the SOFA software allows for multi-material simulation, however, the meshes generated are made by non-uniform elements and are not refined enough to have good results. Furthermore, SOFA uses the *boxROI* function for multi-material modelling, but this is limited to the simulation of cubic and spherical shapes, not including cylindrical or other more complex objects. Lastly, a third way of multi-material modelling that SOFA uses for linear elastic material is based on changing local stiffnesses in the mesh, using the function *localStiffnessFactor*, that defines the proportionality between the Young's modulus of the materials involved in the design. However, as demonstrated in [28], this method is bound to small deformations, as for large deformations hyperelastic material models are required to model soft robotics. For this reason, a geometrical formulation is applied to correct the model.

To resolve all these issues, this paper introduces a new meshing and partitioning algorithm, developed in MATLAB, resulting in a novel technique for the SOFA framework that allows to handle multi-material domains. Furthermore, one of the materials involved in the proposed design of this work is considered hyperelastic and consequently there is no need for a geometric formulation to correct the model in the large deformation regimes. As case study, a cylindrical multi-material actuator is considered. It is composed of an internal chamber, made of an autonomously self-healing hydrogel, and an external reinforcement 3D-printed in TPPU that is not healable [13]. The self-healing polymer, which rely on reversible hydrogen bonds, provides healing capacity in the multi-material actuator.

The paper is structured as follows. In Section III, the actuator design will be presented, explaining in detail the materials involved (Section III-A) and the actuator fabrication (Section III-B). Then, the modelling of the multi-material actuator will be discussed in Section IV, starting from the hydrogel hyperelastic characterization (Section IV-A), with a constitutive law fitted on experimental data, while the TPPU reinforcement is considered linear elastic. Due to the strong adhesion between the two materials, the interaction at interface is considered as a fixed constraint, so the sliding motions are neglected. Then, the MATLAB mesh partitioning algorithm is explained in detail (Section IV-B). At this point, the multi-material SOFA simulation is ready, and the model will be experimentally validated in quasi-static conditions (Section V). To do so, an experimental setup is built and presented in Section V-A, while the results are demonstrating in Section V-B,

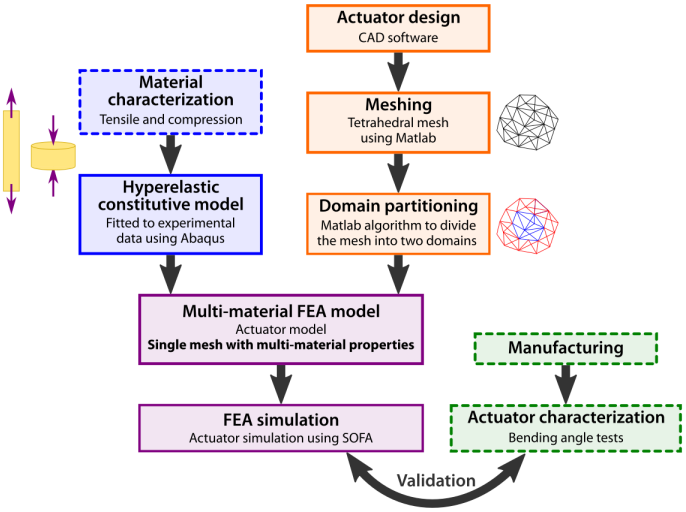

Fig. 1: Methodology followed in this paper to retrieve a FEA-based quasi-static model of a multi-material soft actuator. From materials characterization and the CAD design of the actuator, a multi-material mesh is created using a Matlab algorithm. This model is simulated in SOFA software and its results are compared and validated with the real actuator behaviour. Dashed-line rectangles denote experimental tasks, while solid-line rectangles involve design, modelling or simulation.

showing that the multi-material model built in SOFA matches the reality.

II. Contributions

To highlight the contributions brought to the scientific community on multi-material simulation in SOFA, the novelties of this work are listed:

- The methodology for developing a material-based FEA model from soft robotic actuators presented in [24] is expanded from single material designs towards multi-material soft robotic structures. It involves experimental characterisation of the involved materials, fitting of constitutive material models and implementation in FEA.
- One of the materials involved in the proposed design is modelled as hyperelastic. Consequently the geometrical formulation explained in [28] to correct the SOFA model is not needed, as the simulation matches the reality also in large deformation domain.
- A novel meshing and partitioning technique is developed for the SOFA framework software, involving MATLAB algorithms, that give as output uniform and refined meshes with multiple domains adaptable for any geometry.

III. Actuator design and manufacturing

The pneumatic bending actuator used in this work contains two distinct parts: an internal cylinder-shaped chamber made of a hyperelastic self-healing hydrogel and an external elastic reinforcement (Fig. 2). The inflation of the hyperelastic chamber is constrained on one side by a continuous strip of reinforcement material. the inflation therefore makes the

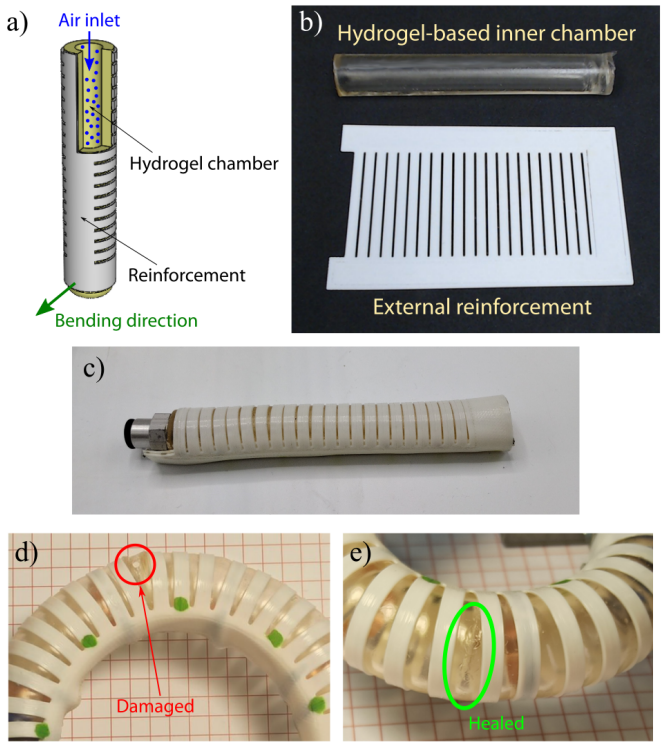

Fig. 2: Design and healing of the multi-material soft pneumatic actuator. a) Schematic view. b) Parts. c) Manufactured actuator. d) Damaged actuator. e) Healed actuator.

actuator bend in one direction. Similar reinforced actuator designs can be found in the literature [29].

A. Materials

The reinformecement in the actuator is a commercial TPPU filament for 3D-printing (Recreus Filaflex® 82A). The hydrogel used for manufacturing the inner chamber of the actuator is an electroactive and self-healable material, of which detailed information on the chemical composition and synthesis can be found in previous work [13], [30]. It is based on a [2-(acryloyloxy)ethyl]-trimethylammonium chloride (AETA) monomer and prepared by photopolymerization under UV light (365 nm) using an exposure of 1-2 minutes. This hydrogel present anti-drying properties and heals autonomously without requiring any external stimulus. In ambient conditions, the hydrogel contains a low amount of water bound to the polymeric chains, situation defined as *equilibrated state*. This water is responsible for the hydrogel self-healing capacity: when two pieces of hydrogel are put together, hydrogen bonds are formed between the water molecules of each side, while still bound to their respective polymeric network, thus causing the healing. This mechanism is detailed comprehensively in [13]. Because of this extraordinary healing function, the actuator can recover completely from being cut and punctured by a sharp object in a matter of minutes (Figs. 2.d, e).

B. Manufacturing

The hydrogel chamber is manufactured by photopolymerization using a transparent mold which consists of two concentric

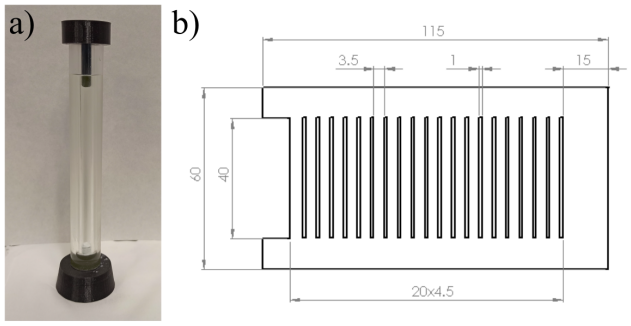

Fig. 3: Actuator manufacturing. a) Mold filled with hydrogel solution to manufacture the chamber. b) Design and dimensions of the 3D-printed reinforcement.

methacrylate tubes (Fig. 3.a). These tubes define the shape of the chamber, with dimensions of 12 mm inner diameter and 21 mm outer diameter. To obtain the chamber, the mold is filled with the hydrogel solution and polymerized using UV light. Next, the part is extracted from the mold and left at ambient conditions for one week to reach the hydrogel equilibrated state. Upon equilibration, the material shrinks due to the loss of water content and as a result the cilindrical chamber shrinks. Eventually the inner diameter is reduced to 10 mm, while the outer diameter reaches 18 mm. It is important to take this volumetric change in account in the design of future healable soft robots manufactured out of this type of self-healing material. The length of the chamber is determined by the quantity of solution poured in the mold and is 115 mm in total, while the inner cavity has a length of 100 mm. The reinforcement is 3D-printed as a planar shape and has a thickness of 0.8 mm (Fig. 3.b). Then the reinforcement structure is rolled over the hyperelastic chamber. Once rolled, the two longitudinal bands of the reinforcement are stuck together using double-sided tape. In this way, thanks to the hydrogel friction and the large compression radial force that the reinforcement is exerting over the hydrogel chamber, both parts are fixed, without the need of adding any adhesive between them.

IV. Multi-material modelling in SOFA

The procedure of making an FEA model of the cylindrical multi-material soft pneumatic actuator starts with a material characterization, including fitting (hyper)elastic material models onto the obtained experimental data of the mechanical properties. Next the geometry has to be meshed, identifying the different material domains and assigning the corresponding properties. Lastly, both the meshed design and the material models are implemented in SOFA, in which the large deformations upon pressurization the actuator are simulated using FEA.

A. Materials characterization

The TPPU, used in the reinforcement, has an almost purely linear elastic characteristic with a Young's Modulus (E) of 45 MPa, Poisson ratio (ν) of 0.39 and density of 1.12 g/cm^3 (values provided by the manufacturing company, Recreus, material

Filaflex® 82A). The hydrogel is hyperelastic as illustrated by Table.I. Uniaxial tensile and compression tests were performed in a Dynamic Mechanical Analyzer (DMA) Q800 of TA Instruments (Fig. 4). For tensile test, a prismatic sample of 5.40 mm length, 5.35 mm width and 1.15 mm thickness were prepared, while a cylindrical sample of 3.65 mm height and 8.20 mm diameter were prepared for compression tests. The two tests were run at 1%/s strain rate, up to 40% strain for the compression tests and up to 250% for the tensile ones, which is a range wide enough for our application. A Poisson ratio (ν) of 0.32 was determined by measuring the transverse strain at multiple points of axial strain (25%, 50%, 75%) and fitting via linear regression ($\nu = -\epsilon_{trans}/\epsilon_{axial}$).

Based on this experimental characterization (stress, strain and Poisson ratio), a hyperelastic constitutive model is fitted using an additional software tool, Abaqus. Multiple constitutive hyperelastic laws were considered in this fitting procedure: Neo-Hookean, Mooney-Rivlin, Yeoh and Ogden (first order). These laws are defined by strain energy density functions (W) that relate the strain energy of a material to its deformation gradient (Table I). Under the assumption of compressibility, isotropy and homogeneity, the relation between the invariants (I_1, I_2, J) of the left Cauchy-Green tensor (B) and the principal stretches (λ_i) can be written as:

$$\lambda_i = 1 + \epsilon_i, \quad i = 1, 2, 3 \tag{1}$$
$$I_1 = \lambda_1^2 + \lambda_2^2 + \lambda_3^2 \tag{2}$$
$$I_2 = \lambda_1^2\lambda_2^2 + \lambda_2^2\lambda_3^2 + \lambda_1^2\lambda_3^2 \tag{3}$$
$$J = \lambda_1\lambda_2\lambda_3 \tag{4}$$
$$\overline{I_1} = J^{-2/3} I_1 \tag{5}$$
$$\overline{I_2} = J^{-4/3} I_2 \tag{6}$$

In which ϵ_i are the principal strains in the three directions. More details about these relations can be found in [24]. From these functions (W), the principal Cauchy stresses (σ_i) can be obtained (more details in [24]). Using this σ_i as function of the principle strain each model can be fitted to the experimental stress-strain data using the Levenberg-Marquardt method. This procedure, carried out in the Abaqus software, provides the results displayed in Fig. 4: stress-strain characteristic of the models compared to the experimental data (Fig. 4.a) and residuals (i.e. errors) between each model and experimental data (Fig. 4.b).

The criteria used to select the suitable material model are the norm of residuals (the lower the better fit) and the Drucker stability of the constitutive law [31]. According to the results shown in Fig. 4 and Table II, the Mooney-Rivlin model can be discarded, while the other three models, the Neo-Hookean, the Yeoh and the Ogden, represent accurately the experimental data and are stable for all strains. The Yeoh model is the most precise as it presents the lowest norm of residuals, but it involves a lot of parameters (see Table I), causing a higher computational cost. For this reason, we decided to select the Neo-Hookean model, as it is accurate but only involves two parameters, leading to a lower computational cost. The fitted values for the Neo-Hookean parameters are $C_{10} = 1.343 \cdot 10^{-2}$ MPa and $D_1 = 30.461$ MPa^{-1}.

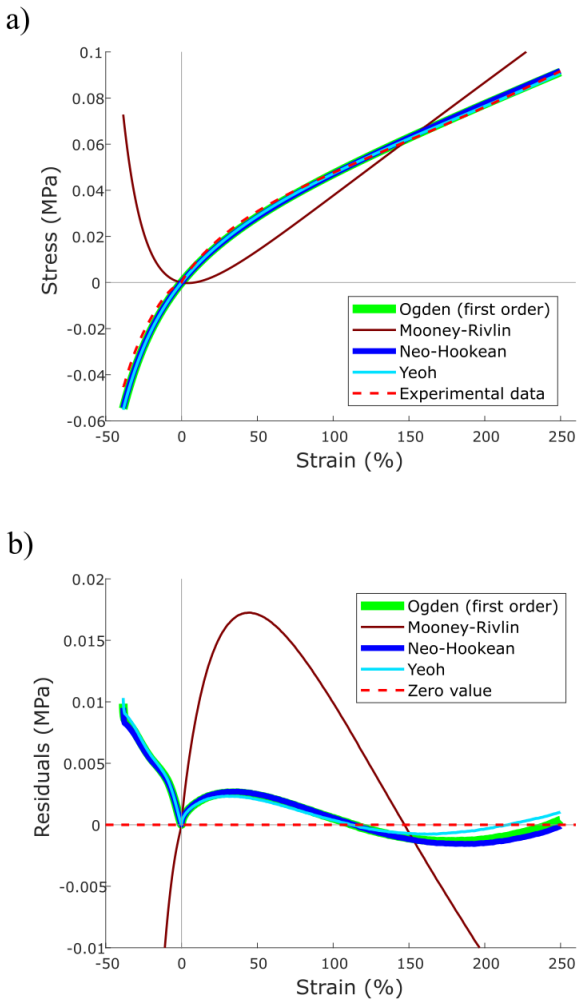

Fig. 4: Fitting of hyperelastic models using experimental data and Abaqus software. a) Stress-strain characteristic. b) Residuals. As can be seen, Ogden, Neo-Hookean and Yeoh models can represent accurately the experimental data, while Mooney-Rivlin is unstable.

B. Mesh and multi-material domain partitioning

Now that we have defined a constitutive law for each of the two materials present in the actuator; a Neo-Hookean model for the hydrogels and a Hookean model for the TPPU, these materials models need to be assigned to the parts of the actuator in the SOFA framework. The multi-material model presented in [28] used the SOFA function *localStiffnessFactor* that makes mesh partitions and varies the material property throughout the design using a proportionality factor on the Young's modulus. This technique works only for linear-elastic materials and is not accurate in large deformation domain in which the hyperelastic behaviour of the hydrogel will be non-negligible. In fact, a geometrical formulation is needed to correct the model. Instead, in this paper, through mesh and multi-material domain partitioning, the hyperelastic model of the hydrogel can be implemented in the multi-material design in SOFA, which permits to reach accurate results also in the

TABLE I: Formula of the strain energy density function (W) for each hyperelastic model considered to fit the hydrogel behaviour.

Model	Strain energy density function, W
Neo-Hookean	$C_{10}(\overline{I_1}-3)+\frac{1}{D_1}(J-1)^2$
Mooney-Rivlin	$C_{10}(\overline{I_1}-3)+C_{01}(\overline{I_2}-3)+\frac{1}{D_1}(J-1)^2$
Yeoh	$C_{10}(\overline{I_1}-3)+C_{20}(\overline{I_1}-3)^2+C_{30}(\overline{I_1}-3)^3+\frac{1}{D_1}(J-1)^2+\frac{1}{D_2}(J-1)^4+\frac{1}{D_3}(J-1)^6$
Ogden	$\sum_{i=1}^{N}\frac{2\mu_i}{\alpha_i^2}(\lambda_1^{\alpha_i}+\lambda_2^{\alpha_i}+\lambda_3^{\alpha_i}-3)+\sum_{j=1}^{N}\frac{1}{D_j}(J-1)^{2j}$

TABLE II: Norm of residuals, root mean square error and Drucker stability for the fitted models over the experimental data.

Model	Norm of residuals [MPa]	RMSE [MPa]	Drucker stability
Neo-Hookean	$9.301\cdot10^{-2}$	$1.829\cdot10^{-3}$	Stable for all strains
Mooney-Rivlin	$76.768\cdot10^{-2}$	$15.105\cdot10^{-3}$	Unstable for all strains
Yeoh	$8.078\cdot10^{-2}$	$1.590\cdot10^{-3}$	Stable for all strains
Ogden (first order)	$8.934\cdot10^{-2}$	$1.758\cdot10^{-3}$	Stable for all strains

large deformation domain, without the need of a geometrical formulation.

In order to obtain simulation results that represent precisely the reality (i.e. experiments), a refined mesh is needed. Furthermore, to do a multi-material simulation, it is essential to distinguish the volumetric parts of the simulated object manufactured with different materials. Although in SOFA, there are *SOFA mesh partitioning tools* that carries out this task, these functions are not used in this work, as they generate meshes that are composed of non-uniform elements and that are not refined. Furthermore, SOFA can use the *boxROI* function that selects all the mesh nodes enclosed in a user defined box, in which is possible to change the material properties. This technique can work for cubic and spherical shapes, but is not available for cylindrical shapes. For these reasons, a MATLAB meshing and partitioning algorithm is developed, resulting in a novel meshing partitioning technique for the SOFA framework. The 3D design was made in Inventor (Autodesk, California, USA), in which the assembly of the hydrogel chamber and the reinforcement was exported as a surface in an STL format, which serves as the input for the MATLAB algoritm. In the simulation, it is assumed that the hydrogel and the TPPU are glued together, e.g. sliding motions at the interface will be neglected. Next, this STL format is imported in MATLAB and using the VTK exportation function, a volume is created with a tetrahedral mesh of 200 thousand elements of uniform dimension to have accurate results and geometry approximation with also a quite good simulation speed of 2.5 FPS. The mesh is exported in VTK format that is compatible with SOFA (a schematic view of the whole process can be seen in Fig. 5.a).

The tetrahedrons that are present in the mesh have to be assigned to one of both domains; the hydrogel or reinforcement material. In the VTK file, we select the mesh elements that have at least three vertices with a higher distance from the longitudinal axis of the cylinder than the external radius of the hydrogel chamber (9 mm). These mesh elements are assigned to the reinforcement domain and the results of this tetrahedrons vertices selection can be seen in red in Fig. 5.b.

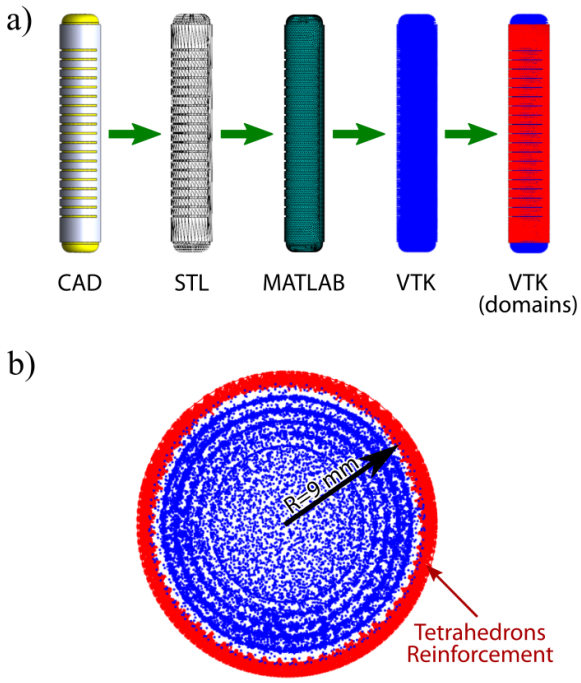

Fig. 5: Meshing and tetrahedrons vertices selection algorithm in the soft pneumatic actuator. a) Series of steps in the procedure. b) Results of tetrahedrons vertices selection (top view); tetrahedrons corresponding to the reinforcement are displayed in red.

C. FEA simulation in SOFA

The mesh that is created in MATLAB and exported in VTK, is imported into SOFA. First of all, the tetrahedrons in the entire mesh are assigned to the hydrogel domain, defined by the hydrogel density and the Neo-Hookean constitutive model that was fitted in a previous section. Then, a sub-topology is created using a *Subset Topological Mapping* which selects the tetrahedrons vertices obtained in the MATLAB algorithm

and updates the properties of these elements by assigning it to the reinforcement domain, defined by the TPPU density and the Hookean linear elastic model. In this way, a multi-material model is created with a Neo-Hookean internal hydrogel chamber and a linear elastic external reinforcement in a unique mesh without considering any sort of constraint between the two parts. Consequently, the entire actuator is completely defined and ready for simulation. The numerical problem is solved using the ODE solver *Euler Implicit Solver* and the *Sparse LDL Linear Solver*.

V. Model validation

In order to validate the multi-material model built in SOFA, the actuator was experimentally characterized in quasi-static conditions.

A. Experimental setup

A dedicated experimental test bench composed of a pressurized air setup and a motion tracking camera is built. The setup is mounted in a plexiglass box of 30×50×50 cm (Fig. 6.a). This box includes a RGBD camera Intel® RealSense™ D435 (element 1 in Fig. 6.a) and a clamp (element 3 in Fig. 6.a) for the pneumatic actuator (element 4 in Fig. 6.a). The soft actuator is actuated using a pressure regulator valve VEAB-L-26-D7-Q4-V1-1R1 from FESTO® (Festo, Esslingen am Neckar, Germany) (element 2 in Fig. 6.a). To control the regulator valve, an Arduino is used. More specifically, a PWM signal is first created and filtered with a low-pass filter. Then, the filtered signal (0 to 5 V) is amplified using an operational amplifier TLC272IP (Texas Instruments, Texas, USA) in order to obtain a 0 to 10 V signal to fit the requirements of the valve control signal. The applied pressure was recorded from the valve using its internal sensor. The sensor signal (0 to 10 V) was passed through a voltage divider to be read by Arduino (0 to 5 V).

The actuator motion is recorded by the camera (element 1 in Fig. 6.a), which was first calibrated using the calibration method described by Zhang *et al.* [32]. Then, the position of the markers fixed on the actuator (Fig. 6.b) can be tracked using real-time color-based segmentation. By doing so, the centroid of each of the blue markers is obtained. Finally, the bending angle (θ) is calculated at every time instant as the angle between the verticle straight line through the base of the actuator (the origin) and the tip of the actuator at rest (along the -Y axis) and a straight line through the base of the actuator and the actuator tip during actuation (Fig. 6.b). In SOFA, six corresponding nodes are selected and their position is tracked during the simulation (Fig. 6.c). In the simulation, the bending angle is calculated as well, in the same way as in Fig. 6.b).

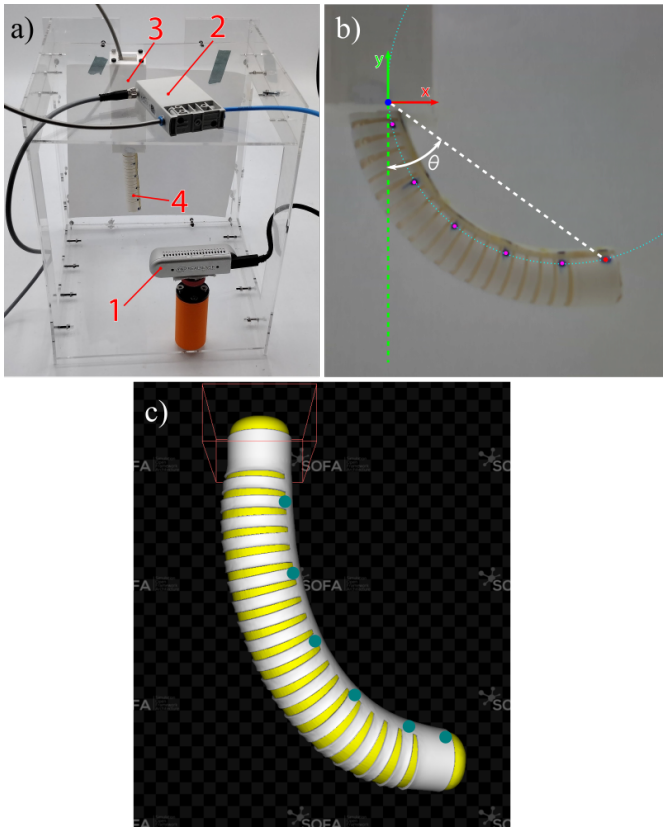

Fig. 6: a) Experimental setup. The camera (1) records the actuator (4), which is hold by a clamp (3) and inflated by a pressure regulator valve (2). b) Bending angle (θ) of the actuator. The centroids of the markers are obtained through the segmentation and are shown in pink, while the last one (tip) is shown in red. The cyan dotted line is a circumference fitted to the markers. c) The SOFA simulation. The markers that are tracked in SOFA are shown in green.

TABLE III: Bending angle expressed in degree for both simulation and experimental results, and RMSE between the simulation markers positions and the experimental ones. All the results are shown for different pressures expressed in bar.

Pressure [bar]	Bending angle [°]		Markers position RMSE [%]
	Simulation	Experimental	
0.10	10.51	9.46	4.2
0.15	15.18	15.18	3.7
0.20	20.43	20.46	3.6
0.25	30.30	28.79	4
0.30	37.02	36.95	3.5
0.35	50.09	50.11	1.8
0.40	65.32	65.48	2.8
0.45	91.23	91.68	4.5

B. Quasi-static tests

In these tests, different pressure levels are introduced in the actuator to compare the corresponding bending behaviour with the simulated one. These tests are performed at discrete pressure values, ranging from 0.10 to 0.45 bar with increments of 0.05 bar, on an actuator which tip is facing downwards at the start of the experiment at 0 bar. The final position of the actuator for each pressure is shown in Fig. 7.a). The position of the selected markers for the experimental tests and simulations at the discrete pressure points are plotted in Fig. 7.b). In Fig. 7.a) and Fig. 7.b), the different colours represent the different pressure level applied. In Fig. 7.c), the bending angle is plotted as a function of the pressure for both the experimental characterization, as well as the simulation.

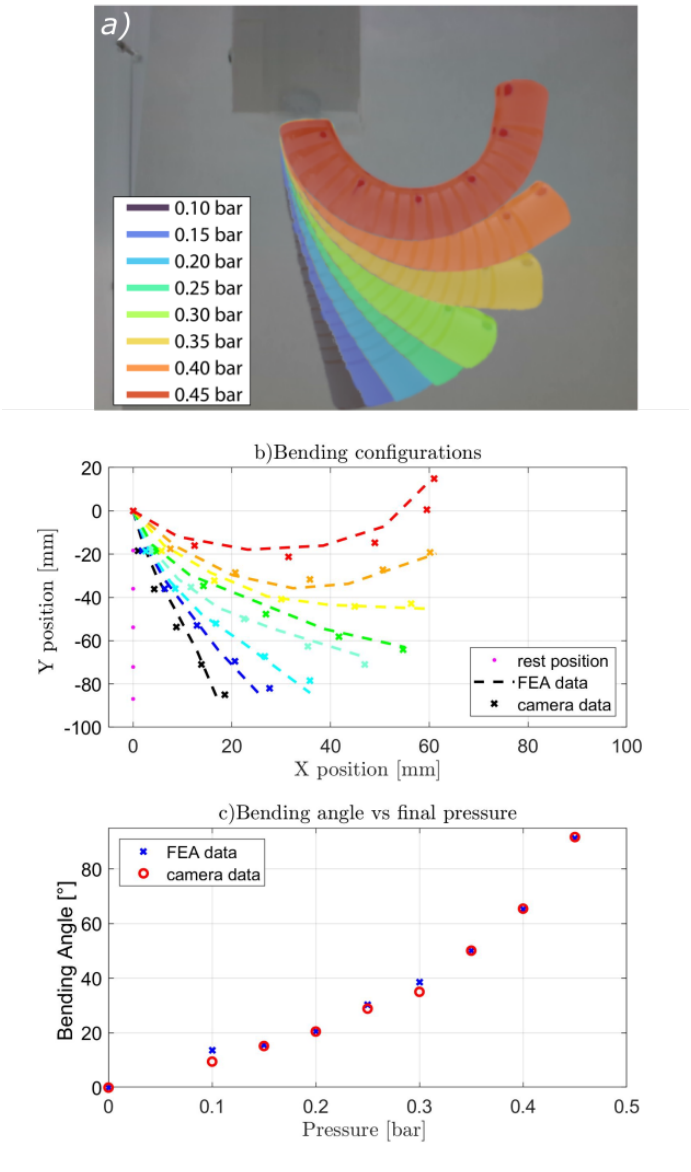

Fig. 7: Quasi-static tests at different pressures. a) Real image of final positions of the actuator. b) Marker positions for experimental tests (crosses) and simulations (dashed line). c) Final bending angle for simulation (blue cross) and experimental data (red circle). All the colors in subfigure b) match the legend shown in a).

As seen in these results, the simulation matches the reality in a accurate way. This is visible from the Fig.7.b), which shows the final markers position tracked both in simulation (dashed lines) and by the camera on the real actuator (crosses). These results are also quantified in Table III, where the simulated bending angles, the experimental ones and the RMSE between the simulated markers positions and the experimental ones are listed for all the quasi-static pressures inputs. The RMSE value are expressed in percent, with respect the total length of the actuator (115 mm). It can be noticed that the RMSE is lower that the 5% for each validation experiment. As visible also in Fig.7.c) the bending angles match for each pressure input. In Fig. 7.c) it is visible that the simulation (dashed lines) and the the experimental bending angle converges to the same values for each pressure input.

VI. Conclusions

In this paper, a quasi-static model for a cylindrical multi-material soft actuator is presented. This FEA model is based on the geometry of the soft robotic actuator and material laws that are fitted onto experimental data derived using uniaxial stress-strain testing. Although the presented approach can be used for any combination of (hyper)elastic materials and any actuator geometry, a self-healing pneumatic bending actuator was selected as a case study. This actuator is composed of an internal self-healing hydrogel based chamber and a 3D printed external reinforcement made in TPPU. The model is made in SOFA, an FEA software that allows interactive simulations.

The paper provide different novel contribution in terms of multi-material simulation using the SOFA framework. This work does not use the traditional multi-material approaches in SOFA, including the mesh partitioning tool or the *boxROI*, because these do not create sufficiently regular meshes and are not adaptable for all geometries. In addition, they do not allow to implement hyperelastic material laws in multi-material designs and are limited to linear elastic modeling. Instead, a MATLAB algorithm is used to generate a unique volumetric mesh with regular tetrahedrons (almost 200 thousand). The mesh is split in two domains, one for hydrogel chamber and one for the TPPU reinforcement. This approach can be used for any geometry and can be expanded to a higher number of domains, when modeling parts that consist out of a large number of materials. It allows to simulate multiple materials via (hyper)elastic material models in the FEA SOFA. Because of this new partition technique, more advanced hyperelastic models can be implemented in multi-material FEA models, increasing the accuracy of these models, in particular for large deformation modes. These (hyper)elastic models can be derived from simple uniaxial material tests. The paper presents a methodology to fit different hyperelastic constitutive laws on experimental data obtained via uniaxial tension and compression tests. Using this approach, a Neo-Hookean model was selected as best fit for the hyperelastic hydrogel, while the TPPU is simulated using a Hookean linear elastic model. Both material models, as well as the partitioned mesh were introduced in SOFA.

The model is experimentally validated in quasi-static conditions. To do this, an actuation setup is built, in which the actuator motion can be tracked during pneumatic actuation, using a camera. For different pressures ranging from 0.1 bar to 0.45 bar the actuation deformations, it was shown that the FEA model outcomes coincide with the experimental characterisation. In fact, the RMSE of selected marker positions between the simulated and experimental marker position are smaller than the 5% of the actuator's total lenght (115 mm) and the simulation and the camera data converge towards the same final bending angle. In conclusion, the quasi-static model can

be considered validated. The authors believe that the accuracy of this material-based quasistatic model results from the precise fitting of the constitutive law on the material level and this for the entire strain window.

ACKNOWLEDGMENT

This research is funded by the EU FET Project SHERO (828818). The FWO (Fonds Wetenschappelijk Onderzoek) funded the work through personal grants of Seppe Terryn (1100416N).

This work is also supported by the EU GA881603-Graphene Core 3 European Union (Flagship project), the Spanish Government (project PID2020-113080RB-I00), the Spanish Ministerio de Educación, Cultura y Deporte (Antonio López-Díaz grant, FPU17/02617) and the FEDER-Junta de Comunidades de Castilla-La Mancha (project SBPL4/17/180501/000204).

REFERENCES

[1] T. George Thuruthel, Y. Ansari, E. Falotico, and C. Laschi, "Control strategies for soft robotic manipulators: A survey," *Soft robotics*, vol. 5, no. 2, pp. 149–163, 2018.

[2] M. R. Cutkosky and S. Kim, "Design and fabrication of multi-material structures for bioinspired robots," *Philosophical Transactions of the Royal Society A: Mathematical, Physical and Engineering Sciences*, vol. 367, no. 1894, pp. 1799–1813, 2009.

[3] D. Guo, Z. Kang, Y. Wang, and M. Li, "Design of multi-material soft pneumatic modules," *Smart Materials and Structures*, vol. 30, no. 9, p. 095006, 2021.

[4] L. Ding, N. Dai, X. Mu, S. Xie, X. Fan, D. Li, and X. Cheng, "Design of soft multi-material pneumatic actuators based on principal strain field," *Materials & design*, vol. 182, p. 108000, 2019.

[5] H. Zhang, A. S. Kumar, F. Chen, J. Y. Fuh, and M. Y. Wang, "Topology optimized multimaterial soft fingers for applications on grippers, rehabilitation, and artificial hands," *IEEE/ASME Transactions on Mechatronics*, vol. 24, no. 1, pp. 120–131, 2018.

[6] C. Aygül, J. Kwiczak-Yiğitbaşi, B. Baytekin, and O. Özcan, "Joint design and fabrication for multi-material soft/hybrid robots," in *2019 2nd IEEE International Conference on Soft Robotics (RoboSoft)*. IEEE, 2019, pp. 477–482.

[7] R. M. Gouker, S. K. Gupta, H. A. Bruck, and T. Holzschuh, "Manufacturing of multi-material compliant mechanisms using multi-material molding," *The international journal of advanced manufacturing technology*, vol. 30, no. 11, pp. 1049–1075, 2006.

[8] S. Terryn, J. Langenbach, E. Roels, J. Brancart, C. Bakkali-Hassani, Q.-A. Poutrel, A. Georgopoulou, T. G. Thuruthel, A. Safaei, P. Ferrentino, T. Sebastian, S. Norvez, F. Iida, A. W. Bosman, F. Tournilhac, F. Clemens, G. V. Assche, and B. Vanderborght, "A review on self-healing polymers for soft robotics," *Materials Today*, vol. 47, pp. 187–205, jul 2021.

[9] Y. J. Tan, G. J. Susanto, H. P. Anwar Ali, and B. C. Tee, "Progress and roadmap for intelligent self-healing materials in autonomous robotics," *Advanced Materials*, vol. 33, no. 19, p. 2002800, 2021.

[10] E. Roels, S. Terryn, F. Iida, A. W. Bosman, S. Norvez, F. Clemens, G. Van Assche, B. Vanderborght, and J. Brancart, "Processing of self-healing polymers for soft robotics," *Advanced Materials*, p. 2104798, 2021.

[11] E. Roels, S. Terryn, J. Brancart, G. Van Assche, and B. Vanderborght, "A multi-material self-healing soft gripper," in *2019 2nd IEEE International Conference on Soft Robotics (RoboSoft)*. IEEE, 2019, pp. 316–321.

[12] S. Terryn, E. Roels, J. Brancart, G. Van Assche, and B. Vanderborght, "Self-healing and high interfacial strength in multi-material soft pneumatic robots via reversible diels–alder bonds," in *Actuators*, vol. 9, no. 2. Multidisciplinary Digital Publishing Institute, 2020, p. 34.

[13] A. Naranjo, C. Martín, A. López-Díaz, A. Martín-Pacheco, A. M. Rodríguez, F. J. Patiño, M. A. Herrero, A. S. Vázquez, and E. Vázquez, "Autonomous self-healing hydrogel with anti-drying properties and applications in soft robotics," *Applied Materials Today*, vol. 21, p. 100806, dec 2020.

[14] R. A. Bilodeau and R. K. Kramer, "Self-healing and damage resilience for soft robotics: a review," *Frontiers in Robotics and AI*, vol. 4, p. 48, 2017.

[15] D. Yuan, S. Delpierre, K. Ke, J.-M. Raquez, P. Dubois, and I. Manas-Zloczower, "Biomimetic water-responsive self-healing epoxy with tunable properties," *ACS applied materials & interfaces*, vol. 11, no. 19, pp. 17 853–17 862, 2019.

[16] M. W. Hannan and I. D. Walker, "Kinematics and the implementation of an elephant's trunk manipulator and other continuum style robots," *Journal of robotic systems*, vol. 20, no. 2, pp. 45–63, 2003.

[17] C. Della Santina, A. Bicchi, and D. Rus, "On an improved state parametrization for soft robots with piecewise constant curvature and its use in model based control," *IEEE Robotics and Automation Letters*, vol. 5, no. 2, pp. 1001–1008, 2020.

[18] Y. Chen, L. Wang, K. Galloway, I. Godage, N. Simaan, and E. Barth, "Modal-based kinematics and contact detection of soft robots," *Soft Robotics*, vol. 8, no. 3, pp. 298–309, 2021.

[19] C. Della Santina, R. K. Katzschmann, A. Biechi, and D. Rus, "Dynamic control of soft robots interacting with the environment," in *2018 IEEE International Conference on Soft Robotics (RoboSoft)*. IEEE, 2018, pp. 46–53.

[20] S. Grazioso, G. Di Gironimo, and B. Siciliano, "A geometrically exact model for soft continuum robots: The finite element deformation space formulation," *Soft robotics*, vol. 6, no. 6, pp. 790–811, 2019.

[21] D. Trivedi, A. Lotfi, and C. D. Rahn, "Geometrically exact models for soft robotic manipulators," *IEEE Transactions on Robotics*, vol. 24, no. 4, pp. 773–780, 2008.

[22] T. G. Thuruthel, E. Falotico, F. Renda, and C. Laschi, "Model-based reinforcement learning for closed-loop dynamic control of soft robotic manipulators," *IEEE Transactions on Robotics*, vol. 35, no. 1, pp. 124–134, 2018.

[23] A. Spielberg, A. Zhao, Y. Hu, T. Du, W. Matusik, and D. Rus, "Learning-in-the-loop optimization: End-to-end control and co-design of soft robots through learned deep latent representations," *Advances in Neural Information Processing Systems*, vol. 32, 2019.

[24] P. Ferrentino, S. K. Tabrizian, J. Brancart, G. Van Assche, B. Vanderborght, and S. Terryn, "Fea based inverse kinematic control on hyperelastic material characterisation of self healing soft robots," *IEEE Robotics and Automation Magazine*, 2021.

[25] C. Duriez, J. Allard, F. Faure, P. Bensoussan, H. Delingette, and S. Cotin, "Ep4a: Software and computer based simulator research: Development and outlook sofa—an open source framework for medical simulation," *Simulation in Healthcare*, vol. 2, no. 4, pp. 284–285, 2007.

[26] C. Duriez, E. Coevoet, F. Largilliere, T. Morales-Bieze, Z. Zhang, M. Sanz-Lopez, B. Carrez, D. Marchal, O. Goury, and J. Dequidt, "Framework for online simulation of soft robots with optimization-based inverse model," in *2016 IEEE International Conference on Simulation, Modeling, and Programming for Autonomous Robots (SIMPAR)*, 2016, pp. 111–118.

[27] K. Wu, G. Zheng, and J. Zhang, "Fem-based trajectory tracking control of a soft trunk robot," *Robotics and Autonomous Systems*, p. 103961, 2022.

[28] G. Fang, C.-D. Matte, R. B. Scharff, T.-H. Kwok, and C. C. Wang, "Kinematics of soft robots by geometric computing," *IEEE Transactions on Robotics*, vol. 36, no. 4, pp. 1272–1286, 2020.

[29] G. Agarwal, N. Besuchet, B. Audergon, and J. Paik, "Stretchable materials for robust soft actuators towards assistive wearable devices," *Scientific reports*, vol. 6, no. 1, pp. 1–8, sep 2016.

[30] A. López-Díaz, A. Martín-Pacheco, A. M. Rodríguez, M. A. Herrero, A. S. Vázquez, and E. Vázquez, "Concentration gradient-based soft robotics: Hydrogels out of water," *Advanced Functional Materials*, vol. 30, no. 46, p. 2004417, sep 2020.

[31] K. Romanov, "The drucker stability of a material," *Journal of Applied Mathematics and Mechanics*, vol. 65, no. 1, pp. 155–162, 2001.

[32] Z. Zhang, "A flexible new technique for camera calibration," *IEEE Transactions on pattern analysis and machine intelligence*, vol. 22, no. 11, pp. 1330–1334, 2000.